Modeling of Semiconductor Detectors Made of Defect-Engineered Silicon: The Effective Space Charge Density

A. Saadoune, S. J. Moloi, K. Bekhouche, L. Dehimi, M. McPherson, N. Sengouga, and B. K. Jones

***Abstract*—The effective space charge density $N_{\rm eff}$ is the average density of carriers over the depletion layer in a semiconductor diode and is measured from the capacitance–voltage curve extrapolated to full depletion $V_{\rm d}$. Full semiconductor modeling has been performed for PIN diodes made of materials with a large density of generation–recombination (g–r) centers, such as irradiated or semi-insulating semiconductors. The results show that this extrapolation method can give incorrect values for the introduction rate of charged traps and g–r centers with large irradiation fluence. This is because the introduction of midgap g–r centers moves the Fermi level toward midgap which allows existing traps to change their ionization state. We propose an alternative approach to evaluate the effective density from the C–V characteristics without the need to evaluate the depletion voltage.**

***Index Terms*—Diode, modeling, radiation damage, semiconductor, semi-insulating.**

I. Introduction

We have been studying the effect of a high density of generation–recombination (g–r) centers on the electrical properties of PIN diodes. These are midgap states which interact approximately equally with the conduction and valence bands. A high concentration of these states changes the material properties from the common lifetime semiconductor [1] to a relaxation semiconductor [2] with different properties. These effects have been studied experimentally [3]–[6] and also by modeling and simulation [7]–[10].

Of particular interest in this work is the fact that, for an intrinsic layer which is initially lightly n-type, the presence of the g–r centers and the generation or recombination of free carriers pulls the Fermi level toward the midgap position [11], [12]. The movement of the Fermi level does not affect the occupation of the shallow donor or acceptor states far away from midgap but have a significant effect on states near midgap.

Manuscript received June 5, 2012; accepted November 26, 2012. Date of publication December 21, 2012; date of current version March 7, 2013. This work was supported by the Agence Nationale pour le Developement de la Recherche Universitaire of Algeria.

A. Saadoune, K. Bekhouche, L. Dehimi, and N. Sengouga are with the Laboratoire des Matériaux Métalliques et Semiconductrices, BP 145, Université de Biskra, Biskra 07000, Algeria.

S. J. Moloi is with the Department of Physics, University of South Africa, Pretoria 0003, South Africa (e-mail: moloisj@unisa.ac.za).

M. McPherson is with the Faculty of Applied Sciences, Cape Peninsula University of Technology, Cape Town 8000, South Africa.

B. K. Jones is with the Department of Physics, Lancaster University, Lancaster LA1 4YB, U.K.

Color versions of one or more of the figures in this paper are available online at http://ieeexplore.ieee.org.

Digital Object Identifier 10.1109/TDMR.2012.2234460

For convenience, we introduce the terminology of Deep Donors (DD) and Deep Acceptors (DA), states that are further away from their respective band edges, as well as Less Deep Donors (LDD) or Less Deep Acceptors (LDA) which are closer to the respective band edges, but are not permanently ionized.

Let us first state the lifetime or textbook result of capacitance measurements. Using the parallel-plate concept [13]

$$C = \frac{\varepsilon_0 K A}{l} \tag{1}$$

where ε_0 is the permittivity of free space, K is the relative permittivity of the dielectric between the plates, A is the plate area, and l is the plate separation. The ac or differential capacitance of the depletion region of a semiconductor is the rate of change of charge with voltage which is approximated [1] as

$$C = \frac{\varepsilon_0 \varepsilon A}{W} \tag{2}$$

where ε is the relative permittivity of the semiconductor, A is now the active area of the depletion region, and W is the width of the depletion region given [4] as

$$\frac{1}{W} = \left[\frac{e n_{\rm t}}{2\varepsilon\varepsilon_0 (V - V_{\rm bi})}\right]^{\frac{1}{2}} \tag{3}$$

where e is the electronic charge, $n_{\rm t}$ is the space charge density which represents the dielectric, and $V_{\rm bi}$ is the built-in voltage. For the case of uniform space charge density, $n_{\rm t}$ is equal to $n_{\rm i}$, the intrinsic carrier density. The diode capacitance is given by substitution of (2) in (3) as

$$\frac{1}{C^2} = \frac{2(V - V_{\rm bi})}{A^2 e n_{\rm i} \varepsilon \varepsilon_0} \tag{4}$$

where A is now the active area of the diode, usually estimated as the size of the detection area. Thus, a plot of $1/C^2$ against V gives the values of $V_{\rm bi}$ and $n_{\rm i}$. For silicon, $V_{\rm bi}$ is about 0.5 V and is usually neglected.

In the case of nonuniform space charge density, we obtain a value for the average or effective $n_{\rm t}$, referred to as $N_{\rm eff}$, if we take the spot value when the capacitance reaches its low saturation or depletion value. At this point, $C = C_{\rm d}$ at $V = V_{\rm d}$ when $W = d$, the full depletion (or geometric) width of the diode. Then

$$V_{\rm d} - V_{\rm bi} = \frac{e d^2 N_{\rm eff}}{2\varepsilon\varepsilon_0} \tag{5}$$

1530-4388/$31.00 © 2012 IEEE

by rearranging (3), where subscript d denotes full depletion. It should be remarked that this textbook result uses many simplifying approximations for the diode and also assumes the simplicity of a lifetime material. A more detailed discussion has been given earlier [9].

II. This Work

The modeling was carried out using the package Kurata [14]. The PIN diode is a $P^+N^-N^+$ structure with a long N^- or intrinsic layer. The structure is divided into M points along the x-axis. A higher density of points was used near the metallurgical junctions. The program uses an explicit integration method to solve the 1-D Poisson, current density, and continuity equations for electrons and for holes using full Shockley–Read–Hall statistics. The variables computed are the electron density n, the hole density p, and the potential V at each mesh point of the structure. Nearly similar work has been done recently [15] on PIN photodiodes.

The initial values of n and p are simply the corresponding doping densities. That is, in the p-region, $p = N_{\rm A}$ and $n = n_i^2/N_{\rm A}$, whereas in the n-region, $n = N_{\rm D}$ and $p = n_i^2/N_{\rm D}$. The boundary conditions are as follows: at the far end of the P^+ contact, $p = N_{\rm A}$, $n = n_i^2/N_{\rm A}$, and $V = 0$ (the reference voltage), whereas at the far end of the N^+ contact, $n = N_{\rm D}$, $p = n_i^2/N_{\rm D}$, and $V =$ the applied voltage. Here, $N_{\rm A}$ and $N_{\rm D}$ are the acceptor and donor densities. A schematic of the sample structure is given later.

The modeling package has been used for other investigations before: the I–V [7], E–V [8], and C–V [9] characteristics. It must be noted that the capacitance calculation requires a different approach for relaxation semiconductors compared with lifetime semiconductors. The calculation is not a simple parallel-plate case, and there are considerable concentrations of free charge carriers. In addition, note that this is a dc or static capacitance.

The experimental results on real samples, particularly those with significant and uncontrolled densities of defects, are found to be frequency dependent because deep traps can respond fully to the ac excitation signal [4], [16], [17]. Because the emission and capture processes are thermally activated as well, there is also corresponding temperature dependence [4], [16], [17]. A comparison with the model should therefore only be made with the low-frequency and/or high-temperature experimental data.

III. Sample

The analysis was carried out for a 350-μm silicon $P^+N^-N^+$ structure with 1×10^{11} cm^{-3} shallow donors (N^-). The nonintrinsic regions are P^+ ($N_{\rm A} = 10^{15}$ cm^{-3}) between 0 and 30 μm and N^+ ($N_{\rm D} = 10^{15}$ cm^{-3}) between 320 and 350 μm. Fig. 1 shows a schematic of the structure.

The sample is long in the sense that much of the excess charge distribution at full depletion is in small areas of the contacts near the junction ends. The contacts are made deep so that there is no significant depletion at $x = 0$ μm and at $x = 350$ μm. We assume sharp metallurgical junctions, mainly

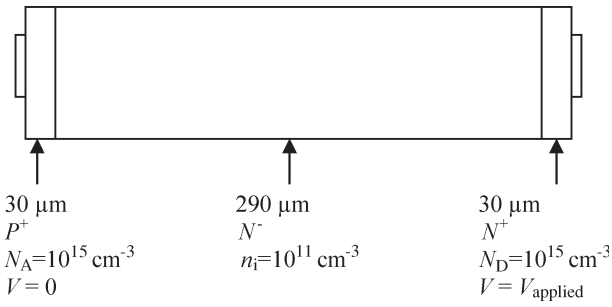

Fig. 1. Schematic of the PIN diode showing the dimensions of the structure and doping densities.

because we have established that the more realistic graded junctions make little difference to the results since the junction region itself is mainly depleted. This means that the details of the contact do not matter much. The temperature was assumed to be 300 K, room temperature.

The intrinsic carrier concentration at room temperature is $n_{\rm i} = 1.45 \times 10^{10}$ cm^{-3}, whereas the dielectric relaxation time is $\tau_{\rm D} \sim 10^{-9}$ s. Thus, the relaxation criterion is reached for a value of the g–r center density of $N_{\rm g-r} \sim 10^{16}$–10^{17} cm^{-3} using $\tau^{-1} = \sigma \upsilon_{\rm th} N_{\rm g-r}$, where $\upsilon_{\rm th}$ is the thermal velocity of carriers. A typical value of 10^{-13} cm^2 is used for the cross section σ [18]–[20], and the centers are at midgap, which is 0.56 eV for silicon, which has $E_{\rm g} = 1.12$ eV. Results of a similar analysis have been given before for the current–voltage characteristics [7]. Although a few parameters are different, a basic behavior of the present simulation can be seen in the results of [7].

In the simulation, the cross sections are set at $\sigma_{\rm n} = \sigma_{\rm p} = 10^{-13}$ cm^2 when the energy is $E_{\rm LDA} = 0.30$ eV for the less deep acceptor. The cross sections are set at $\sigma_{\rm n} = 10^{-14}$ cm^2 and $\sigma_{\rm p} = 10^{-12}$ cm^2 for the deep acceptor at energy of $E_{\rm DA} = 0.70$ eV. It must be noted that $E_{\rm LDA}$ is further away from midgap, whereas $E_{\rm DA}$ is very close. This situation will determine the behavior of the carriers from these traps and, thus, the effective density.

IV. Results and Discussion

The calculations demonstrate various effects which may be observed in real samples. These represent simple special cases because there are too many variables for a wider investigation. The aim of these calculations is to show that, in some cases, care must be taken in the use of $V_{\rm d}$ to obtain $N_{\rm eff}$ and the interpretation of the value obtained. Any conclusions drawn from the results obtained must be emphasized to be approximate. In a similar manner, any modeling results must be interpreted with caution for the mere fact that the model presents simplified cases. The emphasis must be on the use of both results to complement each other in order to attempt to analyze the complex relaxation material.

Let us consider the band diagram of the long PIN diode using a lightly doped n-type material with shallow donors and with a single type of trap. In equilibrium, there is a single Fermi level that is constant throughout the diode. In the (near)

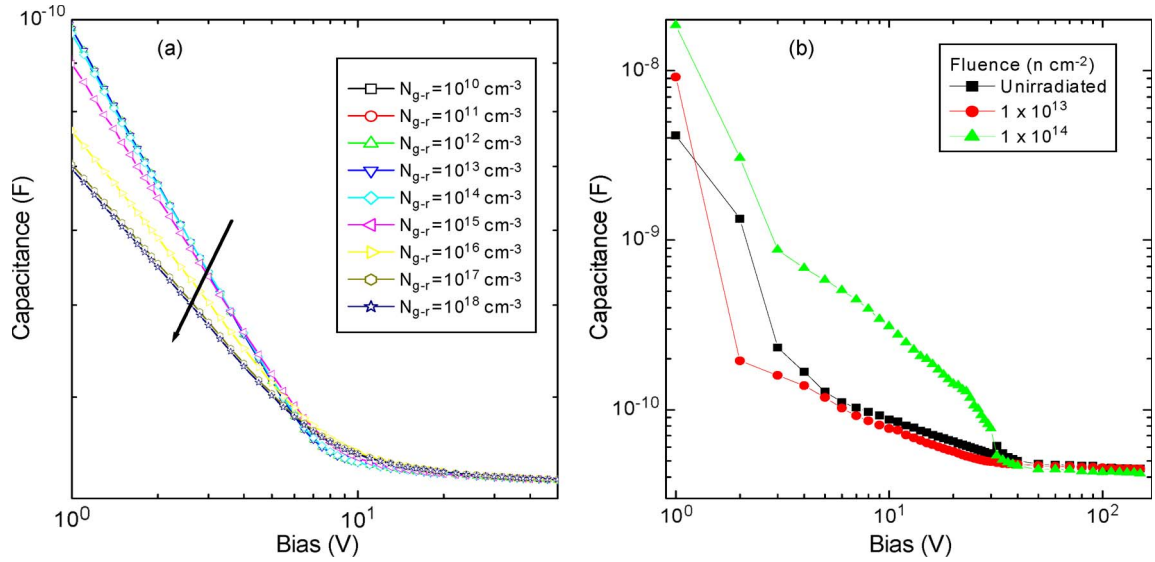

Fig. 2. (a) Calculated C–V characteristics for a diode without any traps, but 10^{11} cm^{-3} shallow donors, as the density of g–r centers increases. (b) Experimental C–V data of an irradiated silicon PIN photodiode.

intrinsic material, the Fermi level is set by the partial ionization of the shallow donors and the traps to give charge neutrality, and the condition is $np = n_i^2$. This condition dominates charge transport in the diode [21].

Once a voltage is applied, the single Fermi level separates into two quasi-Fermi levels. In reverse bias, the hole Fermi level moves up toward the conduction band, whereas the electron Fermi level moves down toward the valence band. As the quasi-Fermi levels separate further, a larger number of traps in the energy gap become positioned above the respective Fermi level [18] and thus become ionized. The reverse bias draws out the ionized free carriers to leave behind ionized fixed traps. In this situation, there are no free carriers.

The value of $V_{\rm d}$ is determined from the fixed traps, whereas that of $N_{\rm eff}$ is found from the free carriers released from these traps. It is worth remarking that $N_{\rm eff}$ is the average trap density as stated earlier. Thus, by definition, $V_{\rm d}$ determines $N_{\rm eff}$ [4]. The opposite is true as well. In a real-life device, this situation becomes complicated by the existence of other impurities that contribute to the current to make the number of free carriers not equal to the number of fixed traps. All types of carriers then contribute to $N_{\rm eff}$.

If there is irradiation, represented by an increased value of $N_{\rm g-r}$, the material tends to relaxation-like; thus, the statistics change, and the conditions become $np = n_i^2$ and $n\mu_{\rm n} = p\mu_{\rm p}$, where μ is the carrier mobility. This condition results in a single Fermi level near midgap. Thus, when the material becomes relaxation-like, we have (using donors as an example) four types of carriers that contribute to the space charge. These are the partially ionized traps between the conduction band and midgap, the less deep donors and less deep acceptors near the band edges, and the free carriers from any point in the band gap that are not fully removed. However, the g–r centers are dominant to pull the Fermi level to midgap [5]. In this case, the Fermi level is not affected anymore by the incident radiation [11]. The material has become radiation hard.

A. C–V Characteristic

The $\log C - \log V$ curves are usually used for a linear extrapolation of the voltage dependence of the capacitance to the saturation or full depletion capacitance. These curves are presented in Figs. 2(a), 4, and 5 for the simulation process for different cases. For comparison purposes, in Fig. 2(b), we present experimental data for two irradiations on a silicon PIN photodiode. If there is a high density of g–r centers and traps, the experimental curve ceases to be linear or has a slope of $-1/2$ expected by the simple theory of a uniformly doped lifetime diode. A peak may appear at low voltages, and the transition to a constant value at high voltages may be gradual. These are expected from the theory of such diodes made from a relaxation material [22].

The increase in the density of g–r centers in Fig. 2(a) corresponds to an increase in radiation damage, and this is shown by the pointer. The curves saturate at each end of the $N_{\rm g-r}$ scale with the most change taking place near $N_{\rm g-r} = 10^{16}$ cm^{-3}. The experimental curve in Fig. 2(b) shows a similar trend with saturation of the capacitance setting in at around 40 V. Below this voltage, the curves are rather noisy, showing the effects of those carriers that are not easily drawn out by the low voltage. However, once saturation has occurred, the sample is at full depletion, and relaxation behavior of silicon ensues.

We have analyzed the data in Fig. 2(a) in a different way to show the saturation and the steep change around the point where relaxation occurs. This analysis is shown in Fig. 3 for a constant V [plot (a)] and for a constant C [plot (b)]. The change in slope occurs because of the high density of free carriers, rather than a fixed ionized donor space charge. The free carriers are $e-h$ pairs generated from g–r centers that cause the relaxation condition. Note that the value of $V_{\rm d}$ does not change much. This is because the generated $e-h$ pairs are easily drawn out by the applied voltage such that they give no net effective space charge at full depletion. Thus, they do not have much of an effect in the bulk.

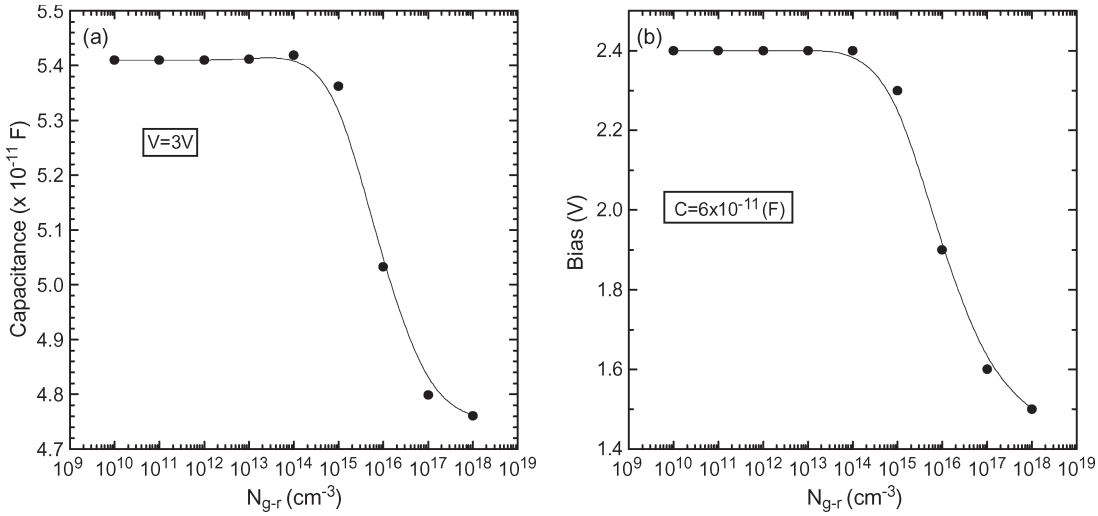

Fig. 3. (a) Calculated $C-N_{\mathrm{g-r}}$ for a constant voltage. (b) $V-N_{\mathrm{g-r}}$ for a constant capacitance derived from Fig. 2(a). The sudden change in either case signifies the point around where relaxation sets in.

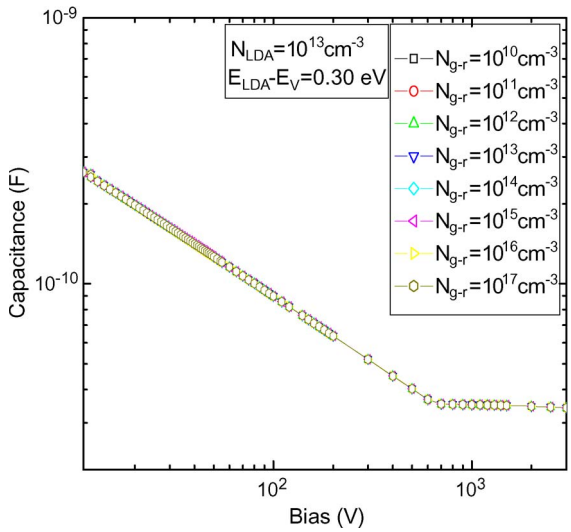

Fig. 4. Change of the C–V characteristics for a concentration of 10^{13} cm^{-3} of a less deep acceptor at $E_{\mathrm{LDA}} = 0.30$ eV as the density of g–r centers increases.

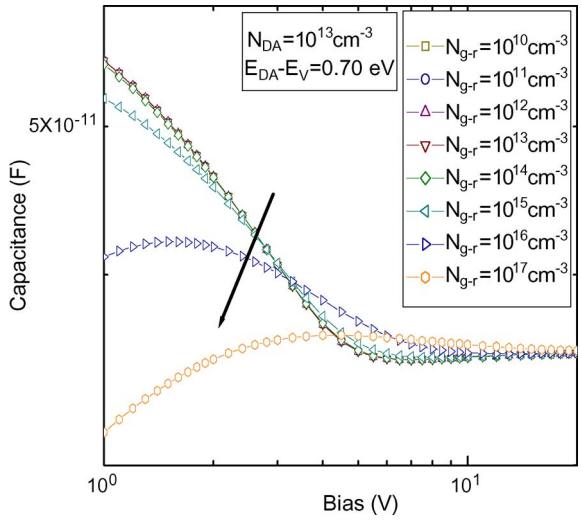

Fig. 5. Change of the C–V characteristics for a concentration of 10^{13} cm^{-3} of a deep acceptor at $E_{\mathrm{DA}} = 0.70$ eV as the density of g–r centers increases.

The saturation on either side of the $N_{\mathrm{g-r}}$ scale is an indication that the effect of radiation is initially not apparent from the plots. This is because, at early stages, the radiation works to reposition the silicon atoms such that interstitials and vacancies are fully occupied. Once this has been achieved at around $N_{\mathrm{g-r}} = 10^{15}$ cm^{-3}, a sudden change takes place when relaxation occurs. After this phase at around $N_{\mathrm{g-r}} = 10^{17}$ cm^{-3}, saturation occurs again. This has been seen before [6], [23] and indicates that irradiation has no effect anymore. This has been also observed for gold-doped diodes [24], [25]. Clearly, it is of no consequence to irradiate the material beyond 10^{17} cm^{-3} nor to dope it beyond the saturation value of gold in silicon. A similar point can be made for other metals like platinum [25].

The increase in the density of g–r centers in Fig. 4 is seen to have no effect on the trend of the measured capacitance. This is because the less deep acceptor at 0.30 eV is completely ionized and also because any g–r centers are created at the g–r position, the midgap. There is no interaction between the g–r centers and the LDA as all charges are drawn out by the applied voltage. In equilibrium, the Fermi level is located close to this level and corresponds to a value of 0.38 eV so that the material is p-type. Since the occupation of this level is not altered much, the value of V_{d} does not change much with $N_{\mathrm{g-r}}$.

In Fig. 5 for the deep acceptor at 0.70 eV, the slope of the C–V characteristic changes, and a peak appears at low voltages for high densities. Unlike in the case of Fig. 4, the density of g–r centers in the case of Fig. 5 has a very significant effect on the trend of the measured capacitance. This effect is clearly seen at low voltages. This is because the acceptor trap is very deep and initially not ionized for a low density of g–r centers. As the density of g–r centers increases, the Fermi level moves to cross the trap level so that this trap level can change its occupation and contribute to the space charge density. For V less than V_{d}, the capacitance is due to the net space charge at the end of the depletion region, and the change in the bulk charges is due to the change in the Fermi levels along the diode. From the simulation

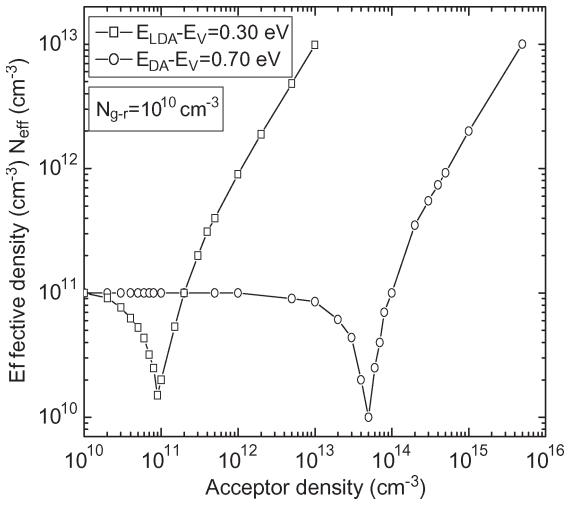

Fig. 6. The effective density $N_{\rm eff}$ is shown in the presence of a less deep acceptor at 0.30 eV and a deep acceptor at 0.70 eV with an increasing density for a sample with a g–r center density of 10^{10} cm^{-3}.

process, it is possible to calculate $V_{\rm d}$ and the corresponding values of $N_{\rm eff}$ as in (5).

The use of (5) is only valid in lifetime semiconductors and for uniform doping. In the present case, we have none of these. The value of $V_{\rm d}$ can be determined from the saturation of the capacitance. However, $N_{\rm eff}$ cannot be evaluated directly from $V_{\rm d}$ because the capacitance is not proportional to $V^{-1/2}$. We suggest using the analysis in Section IV-B [26], [27] to evaluate the space charge density.

B. Effective Density and Type Inversion

Irradiation of a PIN diode with the starting intrinsic material lightly n-type, with no known traps, is found experimentally to produce an initial reduction of $N_{\rm eff}$ and then an increase roughly proportional to the fluence [28]. It is assumed that the radiation damage produces both g–r centers and shallow acceptors which compensate the shallow donor dopants. The material changes its type, and the depletion junction moves to the other end of the intrinsic layer. This is probably a correct assumption, and the type inversion occurs when the new shallow acceptor concentration becomes greater than the original donor concentration. For a trap located close to midgap, type inversion will occur at a fluence of about 10^{13} n cm^{-2} [3], [29].

In some other cases, the above assumption may be seen to give an incorrect conclusion. Consider the results of Fig. 6 for 10^{11} cm^{-3} shallow donor dopants given in Fig. 2 as $n_{\rm i}$ for the N^- region of the PIN structure. For a less deep acceptor at 0.30 eV above the valence band, type inversion occurs at an acceptor density of 9×10^{10} cm^{-3} as the 10^{11} cm^{-3} shallow donor dopants are compensated. However, for the same conditions in the case of a deep acceptor at 0.70 eV, type inversion occurs at an acceptor density of about 5×10^{13} cm^{-3}. This occurs because the deep acceptors are located in the tail of the Fermi–Dirac distribution and not fully ionized when the Fermi level is near midgap. Thus, independent knowledge of the energy of the traps introduced by the irradiation is needed in order to obtain a correct value for the effective density. Below, we suggest a different method for the correct evaluation of $N_{\rm eff}$.

The capacitance of a $p-n$ junction is given by (6) as

$$C = \frac{A\varepsilon\varepsilon_0}{W} \tag{6}$$

which is rearranged to

$$W = \frac{A\varepsilon\varepsilon_0}{C} \tag{7}$$

where the variables are as defined before. Practically, C is calculated as the incremental change of the space charge with respect to an incremental voltage given in

$$dV = W\,dE \tag{8}$$

where dE is the incremental electric field given in terms of the space charge density by Poisson's equation [30] as

$$dE \approx \frac{dQ}{\varepsilon\varepsilon_0} = eN_{\rm eff}(W)\frac{dW}{\varepsilon\varepsilon_0} \tag{9}$$

where the effective space charge density is depletion width dependent. Hence, the incremental voltage of (8) becomes

$$dV = WeN_{\rm eff}(W)\frac{dW}{\varepsilon\varepsilon_0} \tag{10}$$

where $W\,dW$ is written as $1/2d(W^2)$ to give

$$dV = eN_{\rm eff}(W)\frac{d(W^2)}{2\varepsilon\varepsilon_0} \tag{11}$$

and by substitution of (7) into (11), we get

$$dV = eN_{\rm eff}(W)(A\varepsilon\varepsilon_0)^2\frac{d(1/C^2)}{2\varepsilon\varepsilon_0} \tag{12}$$

so that the width-dependent space charge density is given by

$$N_{\rm eff}(W) = 2\cdot\frac{dV}{d(1/C^2)}\cdot(eA^2\varepsilon\varepsilon_0)^{-1} \tag{13}$$

noting that the transformation from (4)–(13) involves the term $(V - V_{\rm bi})/(1/C^2)$ becoming $dV/d(1/C^2)$ with $N_{\rm eff}$ replacing $n_{\rm t}$. If $N_{\rm eff}$ is constant, the slope of $1/C^2$ as a function of V is constant to revert to the lifetime case. If $N_{\rm eff}$ is not constant as is the case in inhomogenously doped diodes, then an average value can be obtained, and this is the relaxation case. This has been discussed in Section IV-A.

We have compared $N_{\rm eff}$ values evaluated by the method of (5) to those evaluated by the method of (13). The two results are presented in Figs. 7 and 8 for the less deep acceptor at 0.30 eV and for the deep acceptor at 0.70 eV, respectively. The plots are simulations of a low density of g–r centers (a) and a high density of g–r centers (b).

For a low density of g–r centers in Fig. 7(a), it can be seen that the simulation results from the two methods coincide. This occurs because the low number of g–r centers is not high enough to turn the lifetime material into a relaxation material. The low number of g–r centers corresponds to the saturation of the capacitance curves at lower values of $N_{\rm g-r}$ shown in Fig. 2.

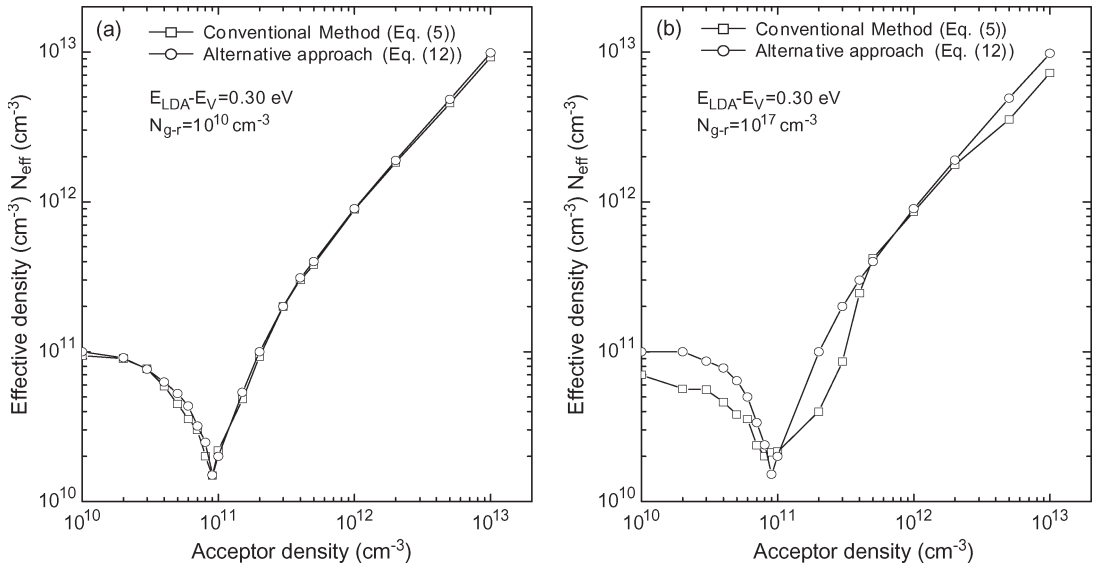

Fig. 7. Comparison of $N_{\rm eff}$ evaluated for a less deep acceptor at 0.30 eV by the conventional method of (5) and by the alternative approach of (13) for (a) a low density (10^{10} cm^{-3}) and (b) a high density (10^{17} cm^{-3}) of g–r centers.

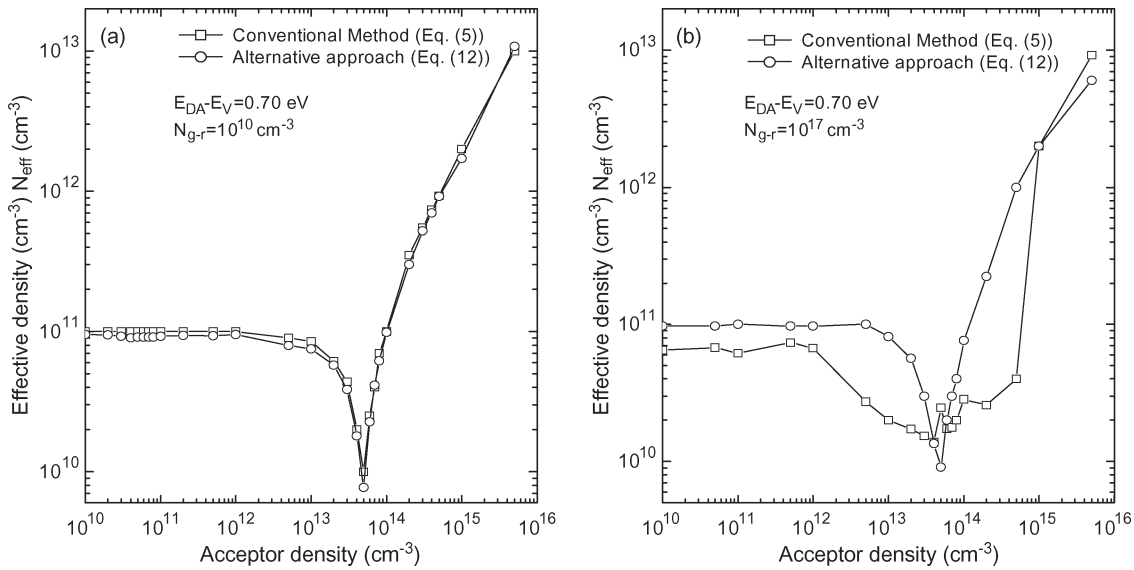

Fig. 8. Comparison of $N_{\rm eff}$ evaluated for a deep acceptor at 0.70 eV by the conventional method of (5) and by the alternative approach of (13) for (a) a low density (10^{10} cm^{-3}) and (b) a high density (10^{17} cm^{-3}) of g–r centers.

For a high density of g–r centers in Fig. 7(b), the two results do not coincide particularly before and just after type inversion. This lack of coincidence arises from the shape of the C–V curve, as shown in Fig. 5, and this does not allow for an easy determination of $V_{\rm d}$. However, the value of $N_{\rm eff}$ evaluated from (13) looks better for two reasons. The first reason is that for a low acceptor density, the value of $N_{\rm eff}$ by (13) is equal to the shallow doping density of 10^{11} cm^{-3}, whereas that evaluated by the usual method of (5) is smaller at 6×10^{10} cm^{-3}. The second reason is that the inversion point determined by (13) appears at a density of an LDA of 9.1×10^{10} cm^{-3}, nearly equal to the shallow doping density, whereas it is smaller (7.6×10^{10} cm^{-3}) in the case of (5).

We must note here that the differences between the two results are so small to be considered negligible. However, it is these small differences that distinguish a lifetime material from a relaxation one. From this perspective then, this new approach is considered highly significant.

In Fig. 8(a), a similar plot is generated for the DA at 0.70 eV and for a low concentration of g–r centers. The simulation results from both methods are coincident, and type inversion occurs at a deep acceptor density of 5×10^{13} cm^{-3}. The occurrence of type inversion is much more agreeable with other works [29], [31]–[34]

In Fig. 8(b), for a high g–r center concentration, the results from (5) are not very good with the material demonstrating an unclear indication of type inversion. This has been also shown in Fig. 6(b) for the LDA. The results obtained from (13) are, however, fairly reasonable with type inversion occurring at the same acceptor density as for the case of low concentration. These results are in agreement with the experimental results of type inversion established some time ago [29], [31]–[34].

Clearly, the method of (5) works for low densities of g–r centers but fails when the irradiation increases. It is then that the method of (13) must be used. The latter is the same equation that is used to determine $N_{\text{eff}}(W)$ for inhomogeneous doping. The only difference between the two is that in the case of (13) before full depletion, the capacitance is due to the change in the net space charge as well as to the change in the bulk charges resulting from the movement of the Fermi levels in the diode. Thus, relaxation in silicon is caused by the activity of any carriers and their mutual interaction, and this is seen by pinning of the Fermi level [5], [35]–[38]

V. Conclusion

Full semiconductor modeling has been performed for a long PIN diode made of silicon material with a large density of g–r centers, such as irradiated or semi-insulating semiconductors to measure the effective space charge density N_{eff}. The results obtained with the conventional method in the presence of a high density of g–r centers are not as expected, and this is due to the fact that the C–V characteristic does not show proportionality to $V^{-1/2}$. Thus, an alternative method is proposed based on (13). The results obtained with the proposed method are better and agree reasonably with the expected results. These simulation results also fit well to experimental results.

Our understanding for practical fabrication of radiation-hard detectors is that the diodes must be made to ensure that the depletion voltage is low at the start and remains low throughout the irradiation. This has been demonstrated with gold before [25], [39] and with other metals [40]. We therefore recommend that appropriate dopants in silicon must be those that can create defects close to midgap as opposed to shallow dopants. The former makes the material already radiation-hard, whereas the latter confuses the analysis and makes the material to behave more intrinsic than relaxation.

Acknowledgment

The authors would like to acknowledge the loan of a package using Kurata and the help of various collaborators in the study of relaxation materials. This work was carried out as part of the CERN RD50 collaboration.

References

[1] S. M. Sze, *Physics of Semiconductor Devices*. New York: Wiley, 1984.
[2] N. M. Haegel, "Relaxation semiconductors: In theory and in practice," *Appl. Phys. A*, vol. 53, no. 1, pp. 1–7, Jul. 1991.
[3] M. McPherson, B. K. Jones, and T. Sloan, "Effects of radiation damage in silicon p-i-n photodiodes," *Semicond. Sci. Technol.*, vol. 12, no. 10, pp. 1187–1194, Oct. 1997.
[4] M. McPherson, "Capacitive effects in neutron-irradiated silicon diodes," *Nucl. Instrum. Methods Phys. Res. A, Accel. Spectrom. Detect. Assoc. Equip.*, vol. 488, no. 1/2, pp. 100–109, Aug. 2002.
[5] M. McPherson, "Fermi level pinning in irradiated silicon considered as a relaxation-like semiconductor," *Phys. B, Condens. Matter*, vol. 344, no. 1–4, pp. 52–57, Feb. 2004.
[6] S. J. Moloi and M. McPherson, "The current and capacitance response of radiation-damaged silicon PIN diodes," *Phys. B, Condens. Matter*, vol. 404, no. 21, pp. 3922–3929, Nov. 2009.
[7] L. Dehimi, N. Sengouga, and B. K. Jones, "Modelling of semi-conductor diodes made of high defect concentration, irradiated, high resistivity and semi-insulating material: The current–voltage characteristics," *Nucl. Instrum. Methods Phys. Res. A, Accel. Spectrom. Detect. Assoc. Equip.*, vol. 519, no. 3, pp. 532–544, Mar. 2004.
[8] L. Dehimi, N. Sengouga, and B. K. Jones, "Modelling of semi-conductor diodes made of high defect concentration, irradiated, high resistivity and semi-insulating material: The internal field," *Nucl. Instrum. Methods Phys. Res. A, Accel. Spectrom. Detect. Assoc. Equip.*, vol. 517, no. 1–3, pp. 109–120, Jan. 2004.
[9] A. Saadoune, L. Dehimi, N. Sengouga, M. McPherson, and B. K. Jones, "Modelling of semi-conductor diodes made of high defect concentration, irradiated, high resistivity and semi-insulating material: The capacitance–voltage characteristics," *Solid State Electron.*, vol. 50, no. 7/8, pp. 1178–1182, Jul./Aug. 2006.
[10] M. A. Cappelletti, U. Urcola, and E. L. Peltzer y Blanca, "Radiation-damaged simulation PIN photodiodes," *Semicond. Sci. Technol.*, vol. 21, no. 3, pp. 346–351, Mar. 2006.
[11] V. N. Brudnyi, S. N. Grinyaev, and V. E. Stepanov, "Local neutrality conception: Fermi level pinning in defective semiconductors," *Phys. B, Condens. Matter*, vol. 212, no. 4, pp. 429–435, Sep. 1995.
[12] B. K. Jones and M. McPherson, "Radiation damaged silicon as a semi-insulating relaxation semiconductor: Static electrical properties," *Semicond. Sci. Technol.*, vol. 14, no. 8, pp. 667–678, Aug. 1999.
[13] A. W. Smith and J. N. Cooper, *Elements of Physics*, 9th ed. New York: McGraw-Hill, 1979.
[14] M. Kurata, *Numerical Analysis for Semiconductor Devices*. Lexington, MA: Lexington Press, 1982.
[15] M. A. Cappelletti, A. P. Cedola, and E. L. Peltzer y Blanc, "Theoretical study of neutron effects on PIN photodiodes with deep-trap levels," *Semicond. Sci. Technol.*, vol. 24, no. 10, p. 105 023, Oct. 2009.
[16] E. Borchi, M. Bruzzi, S. Pirollo, and S. Sciortino, "Temperature and frequency dependence of the capacitance of heavily irradiated silicon diodes," *Solid State Electron.*, vol. 42, no. 11, pp. 2093–2096, Nov. 1998.
[17] D. Campbell, A. Chilingarov, and T. Sloan, "Frequency-temperature scaling of the CV characteristics for irradiated Si detectors," *Nucl. Instrum. Methods Phys. Res. A, Accel. Spectrom. Detect. Assoc. Equip.*, vol. 466, no. 3, pp. 456–463, Jul. 2001.
[18] O. Krasel, C. Gobling, R. Klinenberg, and R. Wunstorf, "Electric fields in irradiated silicon pad detectors," in *Proc. 4th RD50 Workshop CERN*, Geneva, Switzerland, 2004, pp. 1–24.
[19] I. Mandic, M. Batic, V. Cindro, I. Dolenc, G. Kramberger, M. Mikuz, and M. Zavtanik, "CCE of heavily irradiated silicon diodes operated with increased free carrier concentration and under forward bias," in *Proc. 4th RD50 Workshop CERN*, Geneva, Switzerland, 2004, pp. 1–22.
[20] M. McPherson, "Emission and capture processes in radiation-damaged silicon semiconductor diodes," *Current Appl. Phys.*, vol. 2, no. 5, pp. 359–364, Oct. 2002.
[21] B. G. Streetman, *Solid State Electronic Devices*, 3rd ed. London, U.K.: Prentice-Hall, 1990.
[22] B. K. Jones, J. Santana, and M. McPherson, "Negative capacitance effects in semiconductor diodes," *Solid State Commun.*, vol. 107, no. 2, pp. 47–50, May 1998.
[23] P. G. Litovchekov, A. Groza, V. Lastovetsky, L. Barabash, M. Starchik, V. Dubovoy, D. Bisello, P. Giubilato, A. Candelori, R. Rando, A. Litovchenko, V. Khomenkov, W. Wahl, M. Boscardin, N. Zorzi, G. F. Dalla Betta, V. Cindro, M. Mikelsen, E. Monakhov, and B. Svensonn, "Radiation hardness of silicon detectors based on pre-irradiated silicon," *Nucl. Instrum. Methods Phys. Res. A, Accel. Spectrom. Detect. Assoc. Equip.*, vol. 568, no. 1, pp. 78–82, Nov. 2006.
[24] M. McPherson, T. Sloan, and B. K. Jones, "Suppression of irradiation effects in gold-doped silicon detectors," *J. Phys. D, Appl. Phys.*, vol. 30, no. 21, pp. 3028–3035, Nov. 1997.
[25] R. L. Dixon and K. E. Ekstrand, "Gold and platinum doped radiation resistant silicon diode detectors," *Radiat. Protection Dosimetry*, vol. 17, no. 1–4, pp. 527–530, 1986.
[26] A. Saadoune, "Paramétrisation des propriétés électriques d'une diode au silicium soumise à des hautes fluences de particules," Ph.D. dissertation, Univ. Biskra, Biskra, Algeria, 2009.
[27] N. Sengouga, "Hole traps in GaAs FETs: Characterization and back-gating effects," Ph.D. dissertation, Lancaster Univ., Lancaster, U.K., 1991.
[28] M. McPherson, "Irradiated silicon detectors as relaxation devices," Ph.D. dissertation, Lancaster Univ., Lancaster, U.K., 1998.
[29] D. Pitzl, N. Cartiglia, B. Hubbard, D. Hutchinson, J. Leslie, K. O'Shaughnessy, W. Rowe, H. F.-W. Sadrozinski, A. Seiden, E. Spencer, H. J. Ziock, P. Ferguson, K. Holzscheiter, and W. F. Sommer, "Type inversion in silicon detectors," *Nucl. Instrum. Methods Phys. Res. A, Accel. Spectrom. Detect. Assoc. Equip.*, vol. 311, no. 1/2, pp. 98–104, Jan. 1992.
[30] A. Bar-Lev, *Semiconductors and Electronic Devices*, 3rd ed. New York: Prentice-Hall, 1993.

[31] I. E. Anokhin, A. B. Rosenfeld, and O. S. Zinets, "Evolution of radiation induced defects and the type inversion in high resistivity silicon under neutron irradiation," *Radiat. Protection Dosimetry*, vol. 101, no. 1–4, pp. 107–110, 2002.
[32] A. Chilingarov, H. Feick, E. Fretwurst, G. Lindstrom, S. Roe, and T. Schulz, "Radiation studies and operational projections for silicon in the ATLAS inner detector," *Nucl. Instrum. Methods Phys. Res. A, Accel. Spectrom. Detect. Assoc. Equip.*, vol. 360, no. 1/2, pp. 432–437, Jun. 1995.
[33] G. Lindstrom, M. Moll, and E. Fretwurst, "Radiation hardness of silicon detectors—A challenge from high-energy physics," *Nucl. Instrum. Methods Phys. Res. A, Accel. Spectrom. Detect. Assoc. Equip.*, vol. 426, pp. 1–15, 1999.
[34] A. Ruzin, G. Casse, M. Glaser, F. Lemeilleur, R. Talamonti, S. Watts, and A. Zanet, "Radiation hardness of silicon detectors manufactured on epitaxial material and FZ bulk enriched with oxygen, carbon, tin and platinum," *Nucl. Phys. B—Proc. Suppl.*, vol. 78, no. 1–3, pp. 645–649, Aug. 1999.
[35] M. McPherson, "The space charge relaxation behaviour of silicon diodes irradiated with 1 MeV neutrons," *Nucl. Instrum. Methods Phys. Res. A, Accel. Spectrom. Detect. Assoc. Equip.*, vol. 517, no. 1–3, pp. 42–53, Jan. 2004.
[36] J. N. Chazalviel and T. B. Truong, "Quantitative study of Fermi level pinning at a semiconductor–electrolyte interface," *J. Electroanal. Chem.*, vol. 114, pp. 299–303, 1980.
[37] J. M. Palau, A. Ismail, and L. Lassabatere, "Fermi level pinning by interface states: A calculation of the height and the shape of the Schottky barrier," *Solid State Electron.*, vol. 28, no. 5, pp. 499–508, May 1985.
[38] V. L. Berkovits, V. A. Kiselev, T. A. Minashvili, and V. I. Safarov, "Oxidation states and Fermi-level pinning on GaAs(110) surface," *Solid State Commun.*, vol. 65, no. 5, pp. 385–388, Feb. 1988.
[39] M. Msimanga and M. McPherson, "Diffusion characteristics of gold in silicon and electrical properties of silicon diodes used for developing radiation-hard detectors," *Mater. Sci. Eng.—B*, vol. 127, no. 1, pp. 47–54, Feb. 2006.
[40] S. J. Moloi and M. McPherson, "Current–voltage behaviour of Schottky diodes fabricated on *p*-type silicon for radiation hard detectors," *Phys. B, Condens. Matter*, vol. 404, no. 16, pp. 2251–2258, Aug. 2009.

A. Saadoune, photograph and biography not available at the time of publication.

S. J. Moloi, photograph and biography not available at the time of publication.

K. Bekhouche, photograph and biography not available at the time of publication.

L. Dehimi, photograph and biography not available at the time of publication.

M. McPherson, photograph and biography not available at the time of publication.

N. Sengouga, photograph and biography not available at the time of publication.

B. K. Jones, photograph and biography not available at the time of publication.